Microstructure and Mechanical Behaviour of Aluminium Foam Produced by Sintering Dissolution Process Using NaCl Space Holder

Z. Hussain* and N. S. A. Suffin

School of Materials and Mineral Resources Engineering,
Universiti Sains Malaysia, Engineering Campus, 14300 Nibong Tebal,
Pulau Pinang, Malaysia

*Corresponding author: zuhaila@eng.usm.my

Abstract: *In the present work, aluminium foam has been fabricated by sintering an aluminium and NaCl powder mixture followed by a dissolution process. The aim of this research was to study the effect of NaCl space holder content on the morphology and compression properties of aluminium foam. Aluminium foam with porosity in the range of 20–70% and an average pore size of between 400 and 500 μm was produced. Foam produced using 60 wt% NaCl exhibits the highest energy absorption because the foam structure collapsed at higher strain during compression loading. However, 80 wt% NaCl resulted in the foam with the lowest compressive properties and energy absorption because residual NaCl particles caused brittleness.*

Keywords: aluminium foams, sintering dissolution process, compressive properties, energy absorption, compressive deformation mechanisms

1. INTRODUCTION

As a new class of structural materials, metal foams have a good potential in automotive, railway, aerospace and chemical applications, where weight reduction, chemical pollutant minimisation and improvement in comfort and safety are demanded.[1] Metal foams have an extended stress plateau in their compressive stress-strain curves, which is effective for absorbing energy. Currently, there is an increasing interest in using aluminium foams because of their advantages, such as relatively high stiffness despite very low density, high corrosion resistance, excellent noise absorption and vibration suppression and ease of recycling.[2] Thus, aluminium provides environmental and economic benefits to communities and industries across the country. Moreover, aluminium foams that consist of 20–95% pores exhibit superior performance in terms of energy absorption with respect to polymeric foams, despite their greater weight per unit volume.[3] For example, aluminium foams have a range of allowable temperatures that is five times larger than that of polymer foams, which have a maximum temperature limit of approximately 100ºC.[4]

Several methods exist for the manufacture of aluminium foam, namely melt-gas injection, melt-foaming, powder metallurgy, investment casting and melt infiltration.[5] Driven by cost effectiveness and flexibility that leads to designer foams, powder metallurgy has been considered a suitable method for aluminium foam fabrication and has attracted many researchers.[5–7] Zhao and Sun[8] introduced a new development in the powder metallurgy process for aluminium foam fabrication called the sintering dissolution process (SDP), which involves milling, compaction, sintering and dissolution processes. SDP is a process that uses a space holder, which produces an open-cell aluminium foam after dissolving the preform.

Zhihua et al.[10] reported that the elastic modulus and compressive strength of foams depend on the relative density and cell size. Densification strain is sensitive to the relative density; the value decreases with the increase in relative density. Consistent with the findings of Zhihua et al.,[10] Yu et al.[11] observed that the effect of cell size on the compressive and energy absorption properties of aluminium foam can be clearly observed when foams with large cell sizes exhibit an extended plateau in their stress-strain curves, which indicates a higher energy absorption capability. From these studies, it is clear that the compressive properties are influenced by the cell size as well as density of foams.

One of the most difficult tasks in fabricating metallic foams using the SDP method is to obtain a good distribution of pores in the foam structure. The distribution of pores is important because the properties of foam materials depend on their pore structure. Another problem faced during aluminium foam fabrication using SDP is the inhomogeneity of pore shapes because of the strong relationship between morphology and mechanical properties. Jiang et al.[9] claimed that aluminium foams made by SDP may have weaker mechanical properties compared with those fabricated using other techniques, such as infiltration or casting methods. Generally, pore shape is reflected by the shape of the space holder. For example, Mu et al.,[12] who investigated the compressive deformation and failure process in aluminium foams, concluded that pore shape influences the mechanism pore deformation.

Many researchers have investigated the effect of pore shape and seem more interested in rounded space holders to avoid stress formation between the space holder and metallic powder. The amount of space holder used will affect the morphology of foam structures when interconnected pores are formed, which make the pore size become larger. To obtain a foam structure with a tailored morphology distribution, an appropriate space holder must be selected to control the shapes of pores. Jiang et al.[9] fabricated open-cell aluminium foams with porosities between 50% and 80% using carbamide. They found that the pore shape obtained depended on the shape and size distribution of carbamide. Michailidis and Stegioudi[5] also applied the same method using crystalline raw cane sugar to produce open-cell metal foams with porosities in range of 40–70%.

Based on the problems mentioned above, it can be reiterated that the morphology and porosity of aluminium foams depend on the composition of the space holder used in the fabrication process. In this paper, aluminium foam with different cell sizes and densities were fabricated using a NaCl space holder. The aim was to correlate the amount of NaCl to the pore morphology and densities of aluminium foams to improve the compressive properties and energy absorption capability of foams.

2. EXPERIMENTAL

Pure aluminium powder with a purity of 99.8% and particle size of 35 μm was used as the starting material. NaCl with an average particle size of 1 mm was chosen as the space holder. The aluminium powder was mixed thoroughly with the NaCl particles in a ball mill for 1 hour according to the composition ratio listed in Table 1. A small amount of ethanol was added during milling to prevent powder segregation. The mixture was pressed at 200 MPa into a cylindrical compact. The green compact was sintered in a tube furnace at 570ºC under an argon atmosphere for 5 hours of soaking time. The NaCl particles in the sintered aluminium were removed by dissolution in hot water at 90°C for 1 hour.

Table 1: Compositions of mixture powder.

Foam	Al (wt%)	NaCl (wt%)
Al-20NaCl	80	20
Al-40NaCl	60	40
Al-60NaCl	40	80
Al-80NaCl	20	80

The density and porosity of the produced foams were calculated from Equations 1 and 2.[5,6] The structure of the aluminium foams, including cell morphology and microstructure, was examined using a Stereo Zoom optical microscope and Supra 35VP field-emission scanning electron microscope (VPFESEM).

$$Foam\ density,\ \rho_{foam} = \frac{wa}{wc - wb} \times \rho_{liquid} \quad (1)$$

$$Foam\ porosity,\ \rho_{foam} = \left[1 - \left(\frac{pf}{P_{Al}} \right) \right] \times 100\% \quad (2)$$

$$P_{Al} = 2.7g / cm^3,\ P_f = \ foam\ density,\ \rho_{liquid} = 1g / cm^3$$

The compressive properties of the foams were measured using an axial mechanical testing machine at a crosshead speed of 1 mm/min at room temperature. The specimens used for the compression test were 13 mm in diameter and 26 mm in height. The energy absorption of the aluminium foams can be calculated from the area under their stress-strain curves using Equation 3:[13,14]

$$W = \int_0^s \sigma d\varepsilon \quad (3)$$

where W is the energy absorption capability, and σ and ε are the compression stress and strain, respectively.

3. RESULTS AND DISCUSSION

3.1 Density and Porosity of Foams

Figure 1 shows the density and porosity of foams with different NaCl contents. It can be observed that solid aluminium has a higher density compared with aluminium foam. It is clear that the addition of NaCl particles during fabrication reduces the density of aluminium foam. With the dissolution process done in hot water after sintering, the solid aluminium turned into foam through the removal of NaCl particles, as NaCl dissolves in water. The spaces that are created by the NaCl particles become pores, which make the material become lighter. The Al-80NaCl foam exhibited the lowest density and highest porosity compared with other foams. The reduction in density was caused by the presence of a high volume of pores.

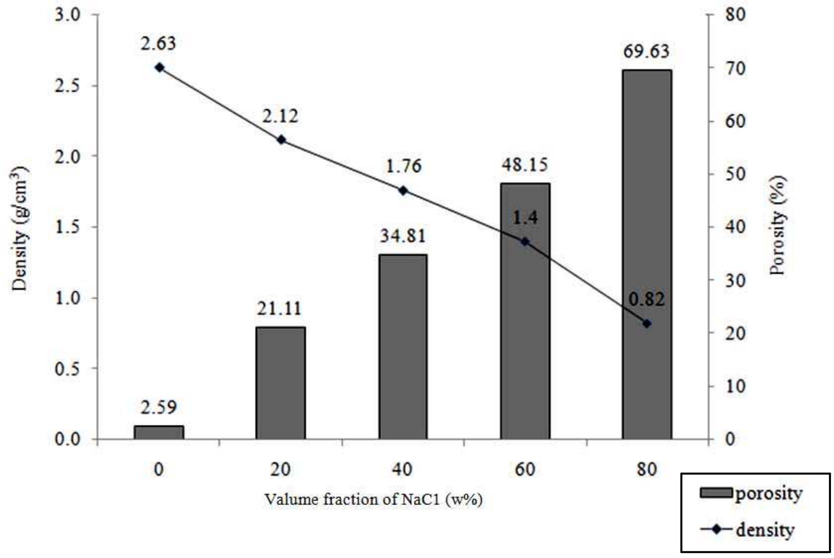

Figure 1: Density and porosity of aluminum foam prepared using different content of NaCl.

3.2 Foam Morphology

It can be seen from Figures 2 and 3 that the foam microstructures vary in pore size and shape. The pore shape replicated the initial cubic shape of the NaCl particles. The following sequence of foam compositions was observed to reflect the pore size in ascending order: Al-20NaCl, Al-40NaCl, Al-60NaCl and Al-80NaCl. From these findings, it is reasonable to infer that by increasing the percentage of NaCl particles, aluminium foams with larger sizes and higher quantities of pores can be obtained. The isolated pores are the most obvious in the Al-20NaCl foam compared with the other foams. As the amount of NaCl increased, interconnected pores were clearly observed, especially in the 20Al-80NaCl foam. This observation indicates that higher space holder contents generate interconnected pores because of the formation of numerous channels between cells, which make foams suitable for absorption applications and components.[15]

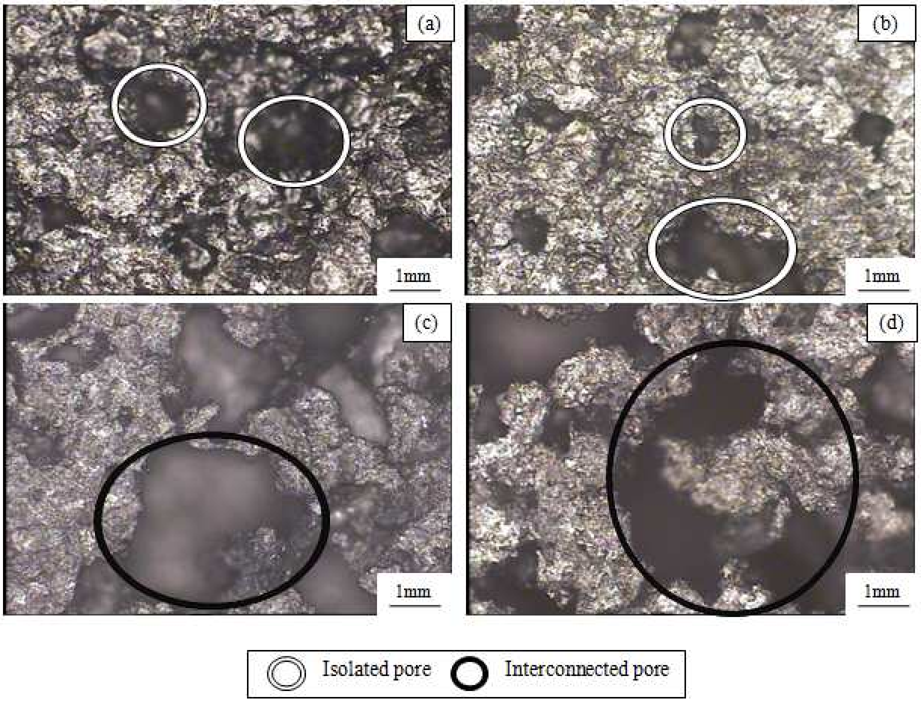

Figure 2: Optical micrograph of typical microscopic structure of Al foam prepared with different content of NaCl: (a) Al-20NaCl; (b) Al-40NaCl; (c) Al-60NaCl; (d) Al-80NaCl.

The relationship between pore size, cell walls and foam density is important to explain the properties of the foams. The characteristics of pores measured from the SEM micrograph shown in Figure 3 are listed in Table 2. Thinner cell walls and larger pore sizes lead to lower foam densities. Thin cell walls developed when large amounts of space holder were used, which led to the formation of closely spaced pores. It has been shown that the Al-80NaCl foam, which had the highest percentage of space holder, had the largest pore size and the smallest wall thickness. As a result, the foam with the lowest density was obtained.

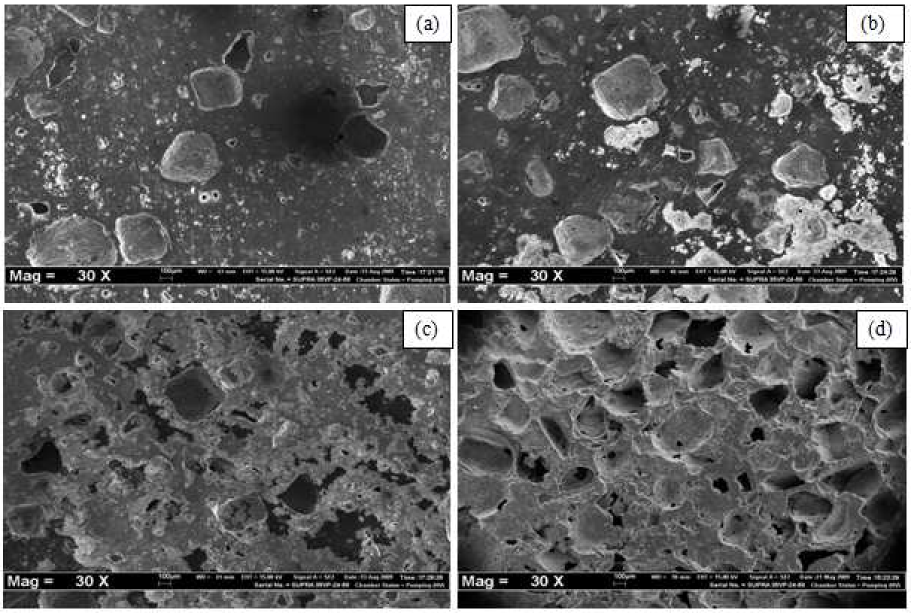

Figure 3: Pore micrograph observation of aluminum foam: (a) Al-20NaCl; (b) Al-40NaCl; (c) Al-60NaCl; (d) Al-80NaCl.

Table 2: Pores characteristic of aluminum foams.

Foam	Al-20NaCl	Al-40NaCl	Al-60NaCl	Al-80NaCl
Density (g/cm^3)	1.99	1.90	1.69	1.30
Average Pore Size (μm)	403.75	422.50	446.86	500.25
Average Wall Thickness (μm)	148.33	117.14	98.57	75.07

3.3 Mechanical Properties

3.3.1 Compressive properties

Figure 4 shows stress-strain curves plotted during compression testing for different aluminium foams prepared using different NaCl particle contents. The stress-strain compression curve can be divided into three stages: (i) linear elastic deformation stage, (ii) plateau deformation stage, and (iii) densification stage. From the stress-strain curves of the foams, the compressive strength, yield stress and modulus can be determined as listed in Table 3. Apparently, increasing the NaCl particle content causes a decrease in the yield strength. The solid aluminium reference curve shows the highest yield strength. As shown in Figure 4, the elastic modulus, which is indicated by the slope of the graph, decreases with the increasing porosity of the foam. This decrease in results is because high porosity elastic deformation may easily occur and results in a reduction in the elastic modulus. Solid aluminium has a higher modulus compared to aluminium foam.

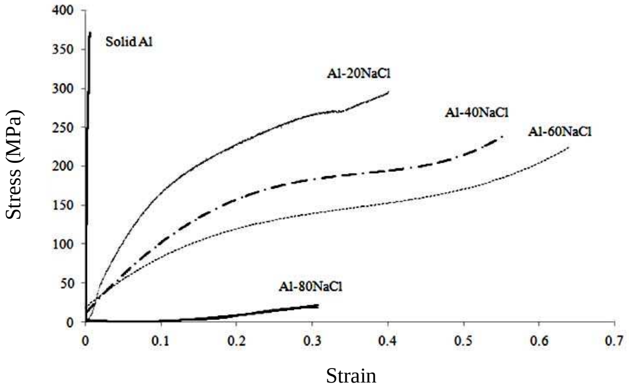

Figure 4: Compressive stress-strain curves of aluminum foam with different percentages of NaCl.

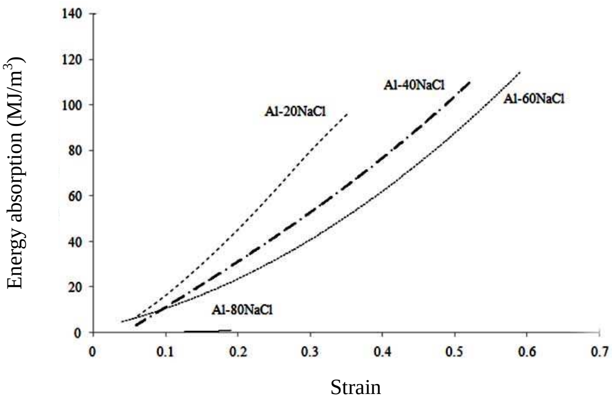

Figure 5: Energy absorption curve of aluminum foam.

Table 3: Stress-strain curve properties of solid aluminum and aluminum foam with various compositions.

Foam	Solid Al	Al-20NaCl	Al-40NaCl	Al-60NaCl	Al-80NaCl
Compressive Strength (MPa)	370.968	271.107	245.692	222.524	19.718
Offset Yield Stress (MPa)	299.056	176.085	144.421	144.455	134.952
Yield Strain	0.004	0.113	0.199	0.354	0.203
Modulus (GPa)	161.262	1.587	0.732	0.410	0.080

In addition, the modulus of the Al-20NaCl foam is much higher (1.587 GPa) compared with Al-80NaCl foam (0.08 GPa). Xiao-qing et al.[16] explained that the pore size of foams influences the elastic modulus in the elastic, plastic plateau and densification regions. In their research, a foam with a small pore size measuring approximately 1.5 mm produced a modulus greater than that of a foam with a larger pore size of 2.5 mm. Similar findings were also reported by Miyoshi et al.,[17] who investigated the mechanical properties of porous aluminium. They revealed that porous aluminium with a small pore size of 1.99 mm showed a higher stress-strain curve than that with a larger pore size of 2.68 mm. In other words, smaller pore sizes would result in foams with greater strengths and moduli. In the present work, the Al-20NaCl foam, which has the lowest composition of NaCl particles showed the highest yield strength and modulus compared with the other foams.

However, the stress-strain curve of the Al-80NaCl foam does not show the typical compression behaviour of foam. The Al-80NaCl foam had the lowest stress-strain curves and failed at lower strain. Foams with high porosity have larger pore sizes and thinner cell walls. Because of this, the Al-80NaCl foam had a weak structure. Thus, the Al-80NaCl foam may have failed because of its thin cell walls. These thin walls could not afford to support the load and caused the structure to collapse, which resulted in failure at low stress. This behaviour is related to the presence of the high density of interconnected pores in the Al-80NaCl foam, which acted as initial cracks in its structure and easily propagated throughout the framework. The plateau stress in this type of foam declines sharply, corresponding to brittle foam behaviour as explained by Bafti and Habibolahzadeh.[6]

3.3.2 Energy absorption

The energy absorption of aluminium foams can be calculated according to Equation 3 for strain ranges between 0.05 and 0.5; the results are shown in Figure 6. It can be seen that the energy absorption capability of the foams grows with increasing strain, though this trend was not observed for the Al-80NaCl foam. This phenomenon shows that the cell structures in the Al-20NaCl, Al-40NaCl and Al-60NaCl foams could support higher stress during mechanical loading before they fractured.

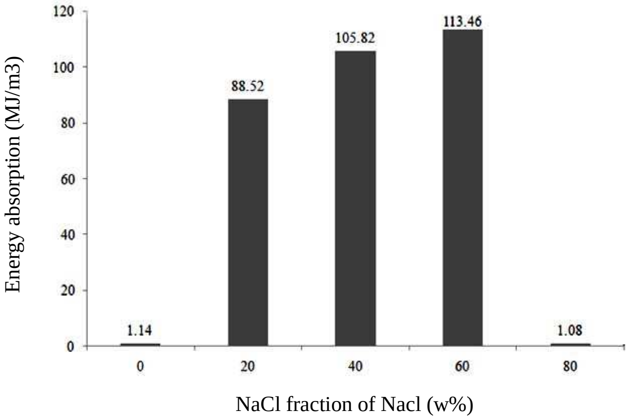

Figure 6: Total energy absorption of aluminum foam.

Figure 6 shows the total energy absorption of the foams during compressive testing. The results were calculated from the area under the stress-strain curves in Figure 4. The Al-80NaCl foam clearly exhibited the lowest energy absorption compared with the other foams, with its value similar to that of solid aluminium. In addition, this foam exhibited brittle behaviour, as indicated by the small area under its stress-strain curve, which corresponds to low energy absorption. This trend may be related to the presence of residual NaCl particles in the Al-80NaCl foam, which were not completely dissolved during the dissolution process. Observation showed that 1 hour of dissolution was not adequate to fully dissolve the amount of NaCl particles in the Al-80NaCl foam. NaCl is an ionic compound that is brittle because of the rigid interactions between charged ions that hold the charged particles in fixed positions.[18] As a brittle material, the remaining NaCl in the aluminium foams affected the properties of the foams. In addition, excessive space holder content caused the cell walls of the foams to become too thin and thus weak. Referring to Table 2 on the morphology observation, Al-80NaCl shows the thinnest cell wall thickness (75.07 μm) compared with the other foams. The weak cell walls of the Al-80NaCl foam did not support further loading during the compression test.

Although the height of the stress-strain curve of the Al-20NaCl foam was the highest, as shown in Figure 4, Figure 6 shows that the cell structures of the Al-20NaCl foam could not support higher loads than those of the Al-40NaCl and

Al-60NaCl foams. According to Figure 6, the energy absorption increased with increasing porosity except for the foam with 80% space holder. This result clearly shows that energy absorption increased from solid aluminium to foams possessing 20%, 40% and 60% space holder, respectively. This result further demonstrates that the Al-60NaCl foam had the highest energy absorption compared with the other foams. This is because the porosity and cell walls of this foam formed a more homogeneous pore structure than the other foams as shown in Figure 3. During compression, a large amount of energy was absorbed during the stages of bending and collapse of the walls in the foam, which occurred mainly along the long stress plateau.[16] Therefore, the microstructure resulted in the Al-60NaCl foam exhibiting better compressive and energy absorption behaviours.

4. CONCLUSION

Using a sintering dissolution process, the fabrication of aluminium foam with porosity in the range of 20–70% can be achieved using NaCl particles with average pore sizes ranging from 400 to 500 μm. Increasing the amount of NaCl powder increases the foam porosity and decreases the foam density due to an increase in the density of interconnected pores. The compressive stress-strain curve of the foam comprises of three regions: linear elastic, plateau and deformation region. The compressive stress-strain curves of the foams fabricated in this study show that there was a decrease in compressive strength with an increase in the amount of incorporated NaCl particles as follows: Al-20NaCl, Al-40NaCl, Al-60NaCl and Al-80NaCl, respectively. This result is due to the presence of residual NaCl particles in the foams. Moreover, because NaCl particles are brittle, they can decrease the compressive strength properties of aluminium foams. However, higher energy absorption was achieved by increasing the amount of NaCl powder, as evidenced by the extended deformation plateau of the foams' stress-strain curves. This result indicates that the Al-60NaCl foam has the highest energy absorption compared with the other foams because of its larger pore size, which supports the Al-60NaCl foam from collapse and thus allows for longer strain during compression loading. However, the Al-80NaCl foam exhibited the lowest compressive properties and energy absorption because of its excessive NaCl particle content, which induced brittleness in the foam.

5. ACKNOWLEDGEMENT

This research was supported by the Universiti Sains Malaysia Short Term Grant 6035290 and Research University Postgraduate Research Student Grant

Scheme of Universiti Sains Malaysia (1001/PBAHAN/8032019). The second author is supported by National Science Fellowship (NSF) from Ministry of Science, Technology and Innovations (MOSTI).

6. REFERENCES

1. Nieh, T. G., Higashi, K. & Wadsworth, J. (2000). Effect of cell morphology on the compressive properties of open cell aluminum foams. *Mater. Sci. Eng. A*, 283(1–2), 105–110.
2. Jeon, Y. P., Kang, C. G. & Lee, S. M. (2009). Effect of cell size on compression and bending strength of aluminum-foamed material by complex stirring in induction heating. *J. Mater. Process. Technol.*, 209(1), 435–444.
3. Ishizaki, K., Komarneni, S. & Nanko, M. (1998). Porous materials: Process technology and applications, 1–44. Dordrecht, Netherlands: Kluwer Academic Publishers.
4. Peroni L., Avalle, M. & Peroni, M. (2008). The mechanical behavior of aluminum foam structures in different loading conditions. *Int. J. Impact Eng.*, 35(7), 644–658.
5. Michailidis, N. & Stergioudi, F. (2011). Establishment of process parameters for producing Al-foam by dissolution and powder sintering method. *Mater. Des.*, 32(3), 1559–1564.
6. Bafti, H. & Habibolahzadeh, A. (2010). Production of aluminum foam by spherical carbamide space holder technique-processing parameters. *Mater. Des.*, 31(9), 4122–4129.
7. Jiang, B., Zhao, N. Q., Shi, C. S., Du, X. W., Li, J. J. & Man, H. C. (2005). A novel method for making open cell aluminum foams by powder sintering process. *Mater. Lett.*, 59(26), 3333–3336.
8. Zhao, Y. Y. & Sun, D. X. (2001). A novel sintering-dissolution process for manufacturing Al foams. *Scr. Mater.*, 44(1), 105–110.
9. Jiang, B., Zhao, N. Q., Shi, C. S. & Li, J. J., (2005). Processing of open cell aluminum foams with tailored porous morphology. *Scr. Mater.*, 53, 781–785.
10. Zhihua, W., Hongwei, M., Longmao, Z. & Guitong, Y. (2006). Studies on the dynamic compressive properties of open cell aluminum alloy foams. *Scr. Mater.*, 54, 83–87.
11. Yu, H., Guo, Z., Li, B., Yao, G., Luo, H. & Liu, Y. (2007). Research into the effect of cell diameter of aluminum foam on its compressive and energy absorption properties. *Mater. Sci. Eng. A*, 454–455, 542–546.
12. Mu, Y., Yao, G., Liang, L., Luo, H. & Zu, G. (2010). Deformation mechanisms of closed cell aluminum foam in compression. *Scr. Mater.*, 63(6), 629–632.

13. Cady, C. M., Gray, G. T., Liu, C., Lovato, M. L. & Mukai, T. (2009). Compressive properties of a closed cell aluminum foam as a function of strain rate and temperature. *Mater. Sci. Eng. A*, 525, 1–6.
14. Yu, S., Liu, J., Wei, M., Luo, Y., Zhu, X., Liu, Y. (2009). Compressive property and energy absorption characteristic of open cell ZA22 foam. *Mater. Des.*, 30, 87–90.
15. Surace, R., De Fhilippis, L. A. C, Ludovico, A. D. & Boghetich, G. (2009). Influence of processing parameters on aluminum foam produced by space holder technique. *Mater. Des.*, 30, 1878–1885.
16. Xiao-qing, C., Zhi-hua, W., Hong-wei, M., Long-mao, Z. & Gui-tong, Y. (2006). Effects of cell size on compressive properties of aluminum foam. *Trans. Nonferrous Met. Soc. China*, 16, 351–356.
17. Miyoshi, T., Itoh, M., Mukai, T., Kanahashi, H., Kohzu, H., Tanabe, S. & Higash K. (1999). Enhancement of energy absorption in a closed-cell aluminum by the modification of cellular structures. *Scr Mater.*, 41(10), 1055–1060.
18. Chemguide. (2000). Ionic structures. Retrieved July 2010, www.chemguide.co.uk.